

# Urban Heat and Urban Cool Islands of Different Land Use Types in Cuiabá, Brazil

**Natallia Sanches e Souza**

Federal University of Mato Grosso

**Marta Cristina de Jesus Albuquerque Nogueira**

Federal University of Mato Grosso

**Flávia Maria de Moura Santos**

Federal University of Mato Grosso

**Luciana Sanches** (✉ [lsanches@hotmail.com](mailto:lsanches@hotmail.com))

Federal University of Mato Grosso <https://orcid.org/0000-0002-3645-3541>

---

## Research Article

**Keywords:** Urban climate, tropical city, urban area, urban expansion areas.

**Posted Date:** November 11th, 2021

**DOI:** <https://doi.org/10.21203/rs.3.rs-506463/v1>

**License:** © ⓘ This work is licensed under a Creative Commons Attribution 4.0 International License.

[Read Full License](#)

---

# Abstract

Urban heat islands (UHIs), urban cool islands (UCIs), and their varying effects due to land use/land cover types and the local climate were investigated from 2014 to 2015 in three urban zones located in Cuiabá city, Brazil, during hot-humid, and hot-dry periods. All the urban zones were analysed for land use/land cover type, local climate, and rate of warming and cooling based on the difference in air temperature ( $\Delta T$ ) between the urban zones and the rural zone located outside the urban perimeter. The annual UHI effect in all the urban zones exhibited varying intensities during the day, with the highest daytime intensity recorded after the sunrise. The duration of UHI effect varied with land use/land cover type; a consequence of high built-up density, verticalization, waterproof surface, and other peculiarities of urban areas. In the urban zones with high built-up density, the duration of UHI effect was observed for up to 24 h, while in the urban areas with low built-up density, the maximum duration of UHI effect was 8 h. On an average, during the daytime, the urban zone with approximately 70% of vegetation cover and water bodies recorded a UCI value of approximately  $-8\text{ }^{\circ}\text{C}$ , whereas the urban zones with approximately 80% waterproof surface and bare land recorded a UCI value close to  $+2\text{ }^{\circ}\text{C}$  during the hot-dry and hot-humid periods. The results indicate that land use and land cover types directly influence UHI intensity.

## 1. Introduction

With rapid urban expansion over the past decades, the green spaces have been replaced by impervious surface such as concrete buildings and highways. These changes in natural land cover alter the thermal properties, surface radiation, and humidity of the urban areas (Meng et al. 2018), resulting in an increase in the Earth's surface temperature, leading to the urban heat island (UHI) effect and urban cool island (UCI) effect, particularly in large cities (Maharjan et al. 2021). Both UHI and UCI represent the rate of warming and cooling based on the difference in air temperature ( $\Delta T$ ) between urban zones and rural zones located outside the urban perimeter.

UHI effect is one of the most studied effects in the urban climate, and can be described as the tendency of the surface air temperature to be higher in the cities than in the surrounding rural areas. The UHI effect can be denoted as the difference in air temperature between the urban and rural areas (Kłysik and Fortuniak 1999), described by Oke (2006) as particular meteorological processes and atmospheric changes that take place in the urban areas.

Many urban patterns can influence the local climate, including the distribution of land use, the design of streets, buildings, and open spaces, as well as the choice of materials; which generate local changes in wind speed and direction, humidity, precipitation, air temperature, dispersion, and deposition of air pollutants (Janković 2013).

The materials used in urban environments play an important role in surface thermal balance. The impact of these materials on the urban atmosphere depends on how they absorb and reflect the incident solar radiation (Monteiro et al. 2021). The major impact of urban heating is on urban land surfaces with more

built-up areas, including paved surfaces (Carnielo and Zinzi 2013). Xie and Li (2021) reported that water bodies in Wuhan were the main contributors to the UCI effect, more than the vegetation cover.

The magnitudes of UHI in different types of local climatic zones vary as the result of surface structure and land cover characteristics of urban canopy layer, which does not always fluctuate continuously in the horizontal space (Zhang et al. 2021). The evaluation of UHI in densely populated cities is crucial to analyse the changes in surface albedo, emissivity, and evapotranspiration.

This paper investigates the UHI and UCI effects due to various land use/land cover types and the local climate in three urban zones in Cuiabá city, Brazil, during hot-humid and hot-dry periods from 2014 to 2015.

## **2. Material And Methods**

### **2.1. Location and description of the study area**

The city of Cuiabá, capital of the state of Mato Grosso (15°35'S and 56°06'W, 165 m), has an area of 3,224.68 km<sup>2</sup>, 254.57 km<sup>2</sup> of urban area and 2,970 km<sup>2</sup> of rural area. It has an estimated population of 618,124 inhabitants with a demographic density of 157.66 inhabitants/km<sup>2</sup> (IBGE 2021). The urban macro-area of Cuiabá is divided into four administrative regions (Fig. 1).

The southern region of Cuiabá has a larger territorial area (128.63 km<sup>2</sup>), whereas the eastern region has a higher population density. According to Köppen climate classification, the regional climate in Cuiabá is classified as Aw, a semi-humid tropical climate with two well-defined seasons: a dry season (autumn–winter) and a rainy season (spring–summer). The average annual precipitation is 1500 mm/year (Sampaio 2006), with dry winters and rainy summers. The predominant wind direction is N (north) and NO (northwest) for most of the year, except S (south) in the winter (Duarte and Serra 2003). Cuiabá is an urban area located in a geographical depression, so the frequency and the average speed of the winds are extremely low. This minimises the effect of thermal exchanges by convection and further emphasises the influence of the built-up space on the air temperature, which generates ideal conditions for experiments with microclimate measurements. Cuiabá has a predominantly hot climate, accentuated by the process of continuous urbanisation that results in high temperatures throughout the year.

### **2.2. Urban Zones**

The selected urban zones in the eastern and western regions of Cuiabá, MT exhibited different characteristics of land cover found in urban areas, and were numbered according to the installed micrometeorological station, as illustrated in Fig. 2.

Urban Zone 1, near meteorological station 1 that was installed in an institutional building, was located close to the Cuiabá River in the eastern region of Cuiabá (Fig. 2).

Urban Zone 2, near meteorological station 2, was located in the Coxipó neighbourhood, an area with lower level of urbanisation than Urban Zone 3, which was located in a residential neighbourhood with high urban density.

## **2.3. Characterization of land use type**

The characterisation and quantification of land use/land cover in the urban areas were defined as green areas, asphalt, water bodies, and buildings using Google Earth images processed in CAD software. The selection of the 200 m radius (Oke 2006) in each area with the scaled image was used to define the land use/land cover type.

## **2.4. Climatic variables**

Air temperature, air humidity, and global solar radiation were measured at four meteorological stations; three of which were installed in an urban area and one in a rural area.

Three 2-m tall micrometeorological towers were installed in the urban area to record the temperature and relative humidity (Model S0THB-M002, ONSET). In order to measure the global solar radiation, a pyranometer (Model S-LIB-M003, ONSET) was connected to a datalogger (Model U30, ONSET) for the storage and remote data transmission.

A 2-m tall micrometeorological tower was installed in a rural area (15°43' S, 56°04' W), and a reference station for heat island analysis was located at a rural farm in the Santo Antônio de Leverger municipality, MT, 15 km from the capital city. It consisted of a datalogger (Model CR1000, Campbell Scientific), and a sensor to measure relative humidity and air temperature (Model HMP45C, Campbell Scientific). The measurements were performed at intervals of 5 min from 8 August 2014 to 20 July 2015.

## **2.5. Urban Heat Island (UHI) and Urban Cool Island (UCI)**

UHI and UCI were calculated by obtaining the differences in surface air temperatures ( $\Delta T$ ) of the urban centres (Urban Zone 1, 2, and 3) in relation to their rural surroundings (Rural Zone), recorded every 30 min. The hot-dry period was considered from 8 August to 30 September 2014 and the hot-humid period was considered from 1 January to 28 February 2015.

## **2.6. Data processing and analysis**

The eventual data gaps detected (failures of less than 5% of the total) were filled out using an artificial neural network with a structure configured by generic algorithms.

After the data gaps were filled, the climatic characterisation of the urban areas was carried out using the hourly average during the month, thus characterising the values of the variables for 24 h a day, called the daily cycle. Similarly, daily cycles for the hot-humid and hot-dry periods were calculated based on the hourly average of the months that comprised of each period.

The hot-dry and hot-humid periods were determined at the beginning of the annual hydrological cycle and the months with total precipitation less than the monthly average of the annual precipitation were considered as the hot-dry period. Thus, in 2014, August, September, and October were considered as the hot-dry period and the rest of the months were classified as the hot-humid period. Similarly, in 2015, May, June, and July were considered as the hot-dry period and January to April were considered as the hot-humid period.

Paired-samples t-tests were conducted to investigate the differences among the UHI intensities across the urban zones. Linear regression analyses were conducted to determine the relationship between environmental variables and UCI values in the urban zones.

### 3. Results And Discussion

#### 3.1. Land use surface classification

The land use type in Urban Zone 1, 2, and 3 was mapped to classify and quantify the land use class (water, built-up, shrubland, underbrush, remnants of vegetation, bare land, concrete, and asphalt) (Fig. 3).

Urban Zones 1, 2, and 3 exhibited similar land use type with variation in percentages. Urban Zone 1 recorded low urbanisation and high vegetation and water cover due to the Cuiabá river’s permanent preservation area (Figs. 3 and 4).

Urban Zone 2 recorded a higher percentage of bare land (24.7%), contributing to the encroachment of the remnants of natural vegetation and urban expansion. This zone did not have all roads paved (Figs. 3 and 4). Urban Zone 3 recorded a high demographic growth and a higher percentage of built-up and urban areas (29.6%), as well as a higher percentage of asphalt pavement (Figs. 3 and 4).

Four categories of land use types in urban zones were identified: waterproof surfaces (buildings and asphalt and concrete pavements), vegetation cover (remnants of natural vegetation, underbrush, and shrubland), bare land, and water surface. Urban Zone 3 recorded the highest percentage of waterproof surfaces, Urban Zone 1 exhibited the highest percentage of vegetation and water surface, and Urban Zone 2 recorded the highest percentage of bare land (Table 1).

Table 1  
Percentages of land use type (waterproof surface, vegetation cover, bare land, and water surface) in Urban Zone 1, 2, and 3 in Cuiabá, MT, Brazil.

| Urban Zone | Waterproof surface | Vegetation cover | Bare land | Water Surface |
|------------|--------------------|------------------|-----------|---------------|
| 1          | 23.5%              | 50.6%            | 8.2%      | 17.7%         |
| 2          | 45.3%              | 29.7%            | 24.7%     | 0.3%          |
| 3          | 74.4%              | 20.0%            | 5.0%      | 0.6%          |

Urban Zone 3 recorded 74.4% of waterproof surface (Table 1) due to the presence of construction materials such as concrete and asphalt, which do not allow water to penetrate and absorb a large amount of heat, thereby increasing the urban temperatures. However, Urban Zone 1 exhibited the largest area under the vegetation cover and water surface (Table 1), which triggered the latent heat transfer process and contributed significantly to attenuating the urban heat.

## **3.2. Micrometeorological analysis during the hot-dry and hot-humid periods**

During the daily cycle, the air temperature tended to be lower from 0 to 5 a.m., which is in contrast to the relative humidity of the air; during the first hours of the day (from 0 to 5 a.m.), it reached its maximum value (Fig. 5).

The maximum air temperature was observed for approximately 14 h, while the relative humidity was recorded at minimum value and was found to be inversely proportional. Similarly, the lowest value of air temperature was recorded at approximately 6 a.m., while the relative humidity was at its peak.

In Urban Zone 1, the difference between the maximum and minimum air temperatures was 8°C during the hot-humid and hot-dry periods, whereas the differences between the maximum and minimum humidity during the hot-humid and hot-dry periods were 28% and 35%, respectively. In Urban Zone 2, the difference between maximum and minimum temperature during the hot-dry and hot-humid periods was 11.5°C and 8.5°C, respectively, whereas the difference between the maximum and minimum humidity during the hot-humid and hot-dry periods was 40% and 32%, respectively. In Urban Zone 3, the difference between the maximum and minimum air temperatures during the hot-dry and hot-humid periods was 11.2°C and 7.4°C, respectively, whereas the difference between the maximum and minimum humidity during the hot-humid and hot-dry periods was 27% and 35%, respectively.

Urban Zone 1, with the highest percentage of vegetation cover and area under water cover, recorded the lowest air temperature. According to Estoque et al. (2017), vegetation cover reduces the land surface temperature due to its low thermal inertia, as it provides shade against sun radiation and generates cool island effects owing to evapotranspiration and emissivity.

Our results of air temperature and relative humidity corroborated the results of climate studies in Cuiabá, MT (Franco 2010; Maciel et al. 2011; Gomes 2012; Oliveira et al. 2012; Luz et al. 2013; Ávila et al. 2015). In Cuiabá, MT, Callejas (2012) and Santos (2012) reported that the thermal amplitude of the hot-dry period was higher than that of the wet period.

Global solar radiation exhibited a similar behaviour with maximum radiation values recorded between 11 a.m. and 12 p.m. (Fig. 6), when the hot-dry and hot-humid periods were analysed with their radiation values according to the daily photoperiod. The incidence of global solar radiation begins at sunrise, which increases until it reaches its peak between 11 a.m. and 12 p.m., and starts decreasing until sunset, around 6 p.m. and 7 p.m.. Maximum radiation values are observed during the hot-humid period.

Variations in global solar radiation across all the urban zones may have been influenced by the locations' characteristics. For example, the Cuiabá River at station 1 favoured higher precipitation, and consequently increased cloudiness.

The minimum values of global solar radiation during the hot-dry period were in accordance with the studies carried out in Cuiabá, MT (Gomes 2010; Maciel et al. 2014), which can be explained by the low relative humidity causing the hot air masses, making it difficult for the global solar radiation to penetrate (Romero 2007).

### **3.3 Urban Heat Island (UHI) and Urban Cool Island (UCI)**

The UHI and UCI intensities can be analysed through the warming and cooling rates in the local climate zones, where a positive  $\Delta T$  indicates an average increase in the surface air temperature (warming) and negative  $\Delta T$  indicates an average decrease in the surface air temperature (cooling).

To understand the behaviour of surface air temperature within a more urbanised area, it is important to analyse the hourly variation of  $\Delta T$  in different seasons, while evaluating the processes that occur throughout the day.

In general, across all the three urban zones,  $\Delta T$  reached its highest values after the sunrise, followed by a rapid change. In Urban Zone 1, the  $\Delta T$  values tended to decrease after the morning period, and the results suggest existence of a  $\Delta T$  with greater intensity within the urban green spaces during the hot-dry period.

This is because during the daytime, urban surfaces absorb more radiation than the urban edges (Monteiro et al. 2021), in this case, the rural areas. In Urban Zone 3, a higher  $\Delta T$  value compared to Urban Zone 2 and Urban Zone 1 was recorded because of the confinement of the reflected radiation between the buildings in urbanised areas. However, in open spaces such as rural areas, a rapid radiative cooling is observed due to no confinement of warm air (Fig. 7, Table 2).

The results demonstrated presence of the UHI effect in all metropolitan areas, with intensities varying according to the period of the day. For example, the UHI intensity had a duration of 4 to 7 h/day during the hot-dry and hot-humid periods, respectively; however, in the urban zone, the UHI intensity had a duration of 15 to 24 h/day. The persistent effect of UCI in local green spaces can be explained by the fact that the monitoring weather station in Urban Zone 1 was installed in areas with high vegetation and surface water cover, leading to a cooling effect due to evapotranspiration and shadows cast by the trees.

In Urban Zone 1, the UCI values exhibited greater amplitude than that of the denser stations as urban configurations, varying between positive and negative values in relation to the average. Moreover, a substantial fraction of negative UHI intensity suggests the existence of a UCI effect.

The intensity of the UHI effect (during the day and night) was calculated considering the daytime from 6 a.m. to 6 p.m. and night-time from 7 p.m. to 5 a.m.

During the daytime, among all the zones, Urban Zone 3 recorded the highest  $\Delta T$  value (Fig. 7) during the hot-dry and hot-humid periods with an approximate average intensity of  $+2.0^{\circ}\text{C}$  and  $+1.3^{\circ}\text{C}$ , respectively; followed by Urban Zone 2 with an average intensity of  $+1.35^{\circ}\text{C}$  and  $+1.0^{\circ}\text{C}$ , indicating a UHI effect. In Urban Zone 1, a negative value of  $\Delta T$  indicating a UCI effect was observed during the hot-dry and hot-humid periods, with an average intensity of  $-7.0^{\circ}\text{C}$  and  $-2.2^{\circ}\text{C}$ , respectively. This reduction in  $\Delta T$  value can possibly be attributed to occupation on the edge areas or greater afforestation in the zone. In general, during the daytime, the three areas presented different energy balances due to the environment's urban characteristics, especially where concrete and asphalt contributed to heat retention. These materials heat up during the day, and then reradiate this heat during the night, making urban temperatures higher than the adjacent rural surroundings (Rizwan et al. 2008).

During the night-time, the Urban Zone 3 recorded the highest UHI value during hot-dry and hot-humid periods, with an average intensity of  $+1.45^{\circ}\text{C}$  and  $+1.05^{\circ}\text{C}$ , respectively. The UHI effect was still present in the zone during the night, possibly due to considerable concrete and asphalt areas.

Much research has been conducted to investigate the effect of increased air temperature on the energy demand of buildings in the urban areas (Kolokotroni 2007). The effect of vegetation cover reduces the heat island values (Kolokotroni et al. 2007; Watkins et al. 2007; Alves 2010) through photosynthesis; the solar energy is used to carry out evapotranspiration, thus avoiding this energy to heat the region (Gartland 2010), and by providing shade (Oliveira et al. 2012). Furthermore, in warmer and drier climates, the effect of vegetation cover is even greater (Lucena 2013).

In Tokyo, Dhakal and Hanaki (2002) reported the implications of anthropogenic heat discharge into the urban environment, and reported the maximum improvement of  $0.47^{\circ}\text{C}$  in mean temperature for the daytime as a result of greening the areas around the buildings.

In a tropical city, Wong and Yu (2005) reported difference between the urban and rural temperature of  $+4^{\circ}\text{C}$ . In Rio de Janeiro, Marques Filho et al. (2009) reported UCI value of approximately 4 to  $5^{\circ}\text{C}$ .

In a study conducted on the island of heat and its influence on the regional climate in the province of Gaungdong, South of China, Chen et al. (2006) found regions of bare land that were warmer than the other land covers. In Brazilian north-eastern cities, Bezerra et al. (2013) reported that the area with the highest urban density recorded higher UHI values, reaching up to  $+7^{\circ}\text{C}$ , compared to areas under vegetation cover.

Due to the high built-up density, verticalization, waterproof surfaces, and other characteristics, the warming effect generated in buildings and the manner in which this heat is exchanged with the ambient environment can play an important role in the urban climate (Krpó et al. 2010). Furthermore, the high demographic growth and urban expansion rates encroach on the last remnants of natural vegetation, contributing to thermal impacts (Oke and Maxwell 1984; Pongracz et al. 2006; Callejas 2012; Callejas et al. 2015).

The highest values of UHI in Cuiabá, MT occurred during the hot-wet period, according to Murphy et al. (2011), who recorded the difference of up to 1 °C between UHI during the hot-humid and hot-dry periods in Puerto Rico.

According to the published UHI values from various tropical cities, the UHI effect is found to be more intense during the morning, reaching its maximum value only before mid-day (Marques et al. 2009; Murphy et al. 2011; Bezerra et al. 2013). This finding is not in agreement with the UHI values recorded in the temperate cities, where it reaches the maximum intensity at night (Oke 1982; Kolokotroni and Giridharan 2008; Van Hove et al. 2015).

A non-parametric t-test was performed to determine a statistically significant difference in UCI in urban zones 1, 2, and 3. The results suggest that the local conditions led to different UCI values with different variances, which proves the relationship between land cover and microclimates formed in each urban zone.

No significant relationship ( $R^2 < 0.43$ ,  $p < 0.05$ ) was observed between the UHI intensity and global solar radiation during the hot-humid and hot-dry periods in urban zones 1, 2, and 3. These results demonstrate the importance of local cloud during a typical wet period and dry fog during the hot-dry period. During the hot-dry period, accumulated particles in the atmosphere are present due to the intense fire events that occur when the native vegetation is burnt in the state of Mato Grosso, Brazil (Dias et al. 2012). Both the effects reduce the incoming global solar radiation.

When the relationship between UHI intensity and air temperature in Urban Zones 2 and 3 was analysed, no significant relationship ( $R^2 < 0.43$ ,  $p < 0.05$ ) during the hot-humid period and hot-dry period was observed. However, a significant relationship ( $R^2 = 0.808$  during the hot-dry period and  $R^2 = 0.783$  during the hot-humid period) was observed in Urban Zone 1.

## Conclusion

The UHI and UCI based on  $\Delta T$  were analysed using in-situ measurements for the three urban and one rural zone in the city of Cuiabá, Brazil. First, these zones were selected, and their land use/land cover types were determined. The daily cycles of meteorological variables and  $\Delta T$  were analysed. Based on the results, the following conclusions can be drawn:

- Local conditions determined different UHI with variances, which proves the relationship between land use/land cover and microclimates formed in each urban zone.
- On an average, all the urban zones exhibited the UHI effect, with intensities varying according to the period of the day, with the highest daytime intensity after sunrise. The duration in hours of UHI varied according to the land use/land cover type, as a consequence of the high built-up density, verticalization, waterproof surface, and other peculiarities of urban areas. In urban zones with high built-up density, UHI could be observed up to 24 h, while in urban areas with low built density, the maximum duration was 8 h.

- On an average, during the daytime, urban zones with approximately 70% of vegetation cover and water surface recorded UCI value close to  $-8\text{ }^{\circ}\text{C}$ . However, the urban zones with approximately 80% of waterproof surface and bare land recorded a UCI close to  $+2\text{ }^{\circ}\text{C}$  during the hot-dry and hot-humid periods.

## Declarations

### Funding

The authors did not receive support from any organization for the submitted work.

### Conflicts of interest/Competing interests.

The authors have no conflicts of interest to declare that are relevant to the content of this article or personal relationships that could have appeared to influence the work reported in this article.

### Availability of data and material (data transparency)

'Not applicable' for that section.

### Code availability (software application or custom code)

'Not applicable' for that section.

### Additional declarations for articles in life science journals that report the results of studies involving humans and/or animals

'Not applicable' for that section.

### Credits

All authors contributed to the study conception and design. Material preparation, data collection and analysis were performed by Natallia Sanches e Souza, Marta Cristina de Jesus Albuquerque Nogueira and Flávia Maria de Moura Santos. The first draft of the manuscript was written by Natallia Sanches e Souza and all authors commented on previous versions of the manuscript. All authors read and approved the final manuscript.

### Ethics approval (include appropriate approvals or waivers)

'Not applicable' for that section.

### Consent to participate (include appropriate statements)

'Not applicable' for that section.

# References

1. Alves EDL (2010) Characterization Microclimatic on the Cuiabá Campus of Mato Grosso Federal University. Dissertation. Federal University of Mato Grosso
2. Ávila AD, Ito CSM, Rocha Triches F, Antunes FF, Amorim Barbosa J, Bissi LB, ... Reichel V (2015) Análise de revestimentos de cobertura do solo em parque urbano na cidade de Cuiabá-MT-Brasil.in: XIII Encontro Nacional e IX Encontro Latino-americano de Conforto no Ambiente Construído. Campinas-SP.
3. Bezerra, PTC, Ramos MDMVB, Leitão PVDA (2013) Heat islands and thermal discomfort in the Brazilian semiarid region: A case study in city of Petrolina-PE. *Revista Brasileira de Geografia Física* 6(03):427-441.
4. Callejas IJA (2012) Avaliação temporal do balanço de energia em ambientes urbanos na cidade de Cuiabá-MT. Thesis. Federal University of Mato Grosso
5. Callejas IJA, Durante LC, Rosseti KDAC (2015) Asphalt paving: Contribution for urban heating areas. *E&S Engineering and Science* 3(1):64-72. <https://doi.org/10.18607/ES201532555>
6. Chen XL, Zhao HM, Li PX, Yin ZY (2006) Remote sensing image-based analysis of the relationship between urban heat island and land use/cover changes. *Remote Sensing of Environment* 104:133-146. <https://doi.org/10.1016/j.rse.2005.11.016>
7. Dhakal S, Hanaki K (2002) Improvement of urban thermal environment by managing heat discharge sources and surface modification in Tokyo. *Energy and Buildings* 34:13-23. [https://doi.org/10.1016/S0378-7788\(01\)00084-6](https://doi.org/10.1016/S0378-7788(01)00084-6)
8. Dias VRM., Sanches L, Alves MC, Souza JN (2012) Spatio-temporal variability of anions in wet precipitation of Cuiabá, Brazil. *Atmospheric Research* 107:9-19. <https://doi.org/10.1016/j.atmosres.2011.11.003>
9. Duarte DHS, Serra GG (2003) Padrões de ocupação do solo e microclimas urbanos na região de clima tropical continental brasileira: correlações e proposta de um indicador. *Ambiente construído* 3(2):7-20.
10. Estoque RC, Murayama Y, Myint SW (2017) Effects of landscape composition and pattern on land surface temperature: An urban heat island study in the megacities of Southeast Asia. *Science of the Total Environment* 577:349-359. <https://doi.org/10.1016/j.scitotenv.2016.10.195>
11. Franco FM (2010) Urban setting and its Interference in Local Microclimate: A Case Study in the District of Porto in Cuiabá-MT. Dissertation. Federal University of Mato Grosso
12. Gartland L (2010) Ilhas de calor: como mitigar zonas de calor em áreas urbanas. Oficina de textos, São Paulo
13. Gomes FD, Sanches L, Alves MDC, Nogueira MDJ, Nogueira JDS (2012) The relationship between meteorological variables and clearness index for four urban/suburban areas of Brazilian cities. *Journal of Environmental Science and Engineering B*(1): 890-900.

14. IBGE - Instituto Brasileiro de Geografia e Estatística. Censo Demográfico (2021). Available in <http://www.ibge.gov.br/> last accessed 10/03/2021
15. Janković V (2013) A historical review of urban climatology and the atmospheres of the industrialized world. *Wiley Interdiscip. Rev. Clim. Chang.* 4:539-553. <https://doi.org/10.1002/wcc.244>
16. Kłysik K, Fortuniak K (1999) Temporal and spatial characteristics of the urban heat island of Łódź, Poland. *Atmospheric environment* 33(24-25):3885-3895. [https://doi.org/10.1016/S1352-2310\(99\)00131-4](https://doi.org/10.1016/S1352-2310(99)00131-4)
17. Kolokotroni M, Giridharan, R (2008) Urban heat island intensity in London: An investigation of the impact of physical characteristics on changes in outdoor air temperature during summer. *Solar energy* 82(11):986-998. <https://doi.org/10.1016/j.solener.2008.05.004>
18. Kolokotroni M, Zhang Y, Watkins R (2007) The London heat island and building cooling design. *Solar Energy* 81(1):102-110. <https://doi.org/10.1016/j.solener.2006.06.005>
19. Krpo A, Salamanca F, Martilli A, Clappier A (2010) On the impact of anthropogenic heat fluxes on the urban boundary layer: a two-dimensional numerical study. *Boundary-layer meteorology* 136(1):105-127. <https://doi.org/10.1007/s10546-010-9491-2>
20. Lucena AJ, Rotunno Filho OC, Almeida França JR, Faria Pere, L, Xavier LNR (2013) Urban climate and clues of heat island events in the metropolitan area of Rio de Janeiro. *Theoretical and applied climatology* 111(3):497-511. <https://doi.org/10.1007/s00704-012-0668-0>
21. Luz VS, Maciel CR, Pinto Júnior OB, Nogueira MCDJA, Nogueira JS (2013) Análise preliminar das características ambientais em espaço de lazer: pista de caminhada da UFMT. *Revista Eletrônica em Gestão, Educação e Tecnologia Ambiental* 9(9):2049-2058. <http://dx.doi.org/10.5902/2236117077009>
22. Maciel CR, Luz VS, Santos FMM, Nogueira MCDJA, Nogueira JS (2014) Interaction of microclimatic variables and ground cover at urban and limitrophe-urban area in the city of Cuiabá-MT. *Caminhos de Geografia* 15(51).
23. Maciel CR, Nogueira MCDJA, Nogueira JS (2011) Ground cover and its influence on temperature of urban microclimate of Cuiabá-MT. *Caminhos de Geografia* 12(39).
24. Maharjan M, Arya A, Man Shakya B, Talchabhadel R, Thapa BR, Kumar S (2021) Evaluation of Urban Heat Island (UHI) Using Satellite Images in Densely Populated Cities of South Asia. *Earth*, 2(1):86-110. <https://doi.org/10.3390/earth2010006>
25. Marques Filho EP, Karam HÁ, Miranda AG, Franca JRA (2009) Rio de Janeiro's urban climate. *Urban Climate News - Quarterly Newsletter of the International Association of Urban Climate (IAUC)* 32:5-9.
26. Meng Q, Zhang L, Sun Z, Meng F, Wang L, Sun Y (2018) Characterizing spatial and temporal trends of surface urban heat island effect in an urban main built-up area: A 12-year case study in Beijing, China. *Remote Sens. Environ.* 204:826-837. <https://doi.org/10.1016/j.rse.2017.09.019>
27. Monteiro FF, Gonçalves WA, Andrade LDMB, Villavicencio LMM, dos Santos Silva CM (2021) Assessment of Urban Heat Islands in Brazil based on MODIS remote sensing data. *Urban Climate* 35: 100726. <https://doi.org/10.1016/j.uclim.2020.100726>

28. Murphy DJ, Hall MH, Hall CA, Heisler GM, Stehman SV, Anselmi-Molina C (2011) The relationship between land cover and the urban heat island in northeastern Puerto Rico. *International Journal of Climatology* 31(8):1222-1239. <https://doi.org/10.1002/joc.2145>
29. Oke TR (1982) The Energetic Basis of the Urban Heat Island. *Quarterly Journal of the Royal Meteorological Society* 108(455):1-24.
30. Oke TR (2006) Initial guidance to obtain representative meteorological observations at urban sites. IOM Report, TD. World Meteorological Organization.
31. Oke TR, Maxwell GB (1984) Urban heat island dynamics in Montreal and Vancouver. *Journal of Climatology* 9:192-200.
32. Oliveira AS, Nogueira MCJA, Sanches L, De Muis CR (2012) Urban microclimate – public squares in Cuiabá/MT/BR/Brazil. *Revista Caminhos de Geografia* 13(43): 311-325.
33. Pongracz R, Bartholy J, Dezso Z (2006) Remotely sensed thermal information applied to urban climate analysis. *Advances in Space Research* 37:2191-2196. <https://doi.org/10.1016/j.asr.2005.06.069>
34. Rocha AF, Paula DCJ, Souza NS, Silva PCBS, Miranda AS, Zamadei T, Souza AP, Machado N. G, Santos, FMM, Nogueira JS, Nogueira MCJA (2015) Variações microclimáticas de áreas urbanas em biomas no estado de Mato Grosso: Cuiabá e Sinop. *Revista Gestão & Sustentabilidade Ambiental* 4:246-257.
35. Romero MAB (2007) *Arquitetura bioclimática do espaço público*. 1. ed. Brasília: UNB, 226 p.
36. Sampaio MMA (2006) An analysis of thermal and lighting factors in low-cost housing in Cuiabá, Mato Grosso. Dissertation. Federal University of Mato Grosso
37. Santos FMM (2012) Influence of land use change in the thermo-hygrometric in Cuiabá-MT. Thesis, Federal University of Mato Grosso
38. Van Hove LWA, Jacobs CMJ, Heusinkveld BG, Elbers JA, Van Driel BL, Holtslag, AAM (2015). Temporal and spatial variability of urban heat island and thermal comfort within the Rotterdam agglomeration. *Building and Environment* 83:91-103. <https://doi.org/10.1016/j.buildenv.2014.08.029>
39. Watkins R, Palmer J, Kolokotroni M (2007) Increased temperature and intensification of the urban heat island: Implications for human comfort and urban design. *Built Environment* 33(1): 85-96. <https://doi.org/10.2148/benv.33.1.85>
40. Wong NH, Yu C (2005). Study of green areas and urban heat island in a tropical city. *Habitat International* 29(3): 547-558. <https://doi.org/10.1016/j.habitatint.2004.04.008>
41. Xie Q, Li J (2021) Detecting the Cool Island Effect of Urban Parks in Wuhan: A City on Rivers. *International Journal of Environmental Research and Public Health* 18(1): 132. <https://doi.org/10.3390/ijerph18010132>
42. Zhang Y, Zhang J, Zhang X, Zhou D, Gu Z (2021) Analyzing the Characteristics of UHI (Urban Heat Island) in Summer Daytime Based on Observations on 50 Sites in 11 LCZ (Local Climate Zone) Types in Xi'an, China. *Sustainability* 13(1):83. <https://doi.org/10.3390/su13010083>

43. Carnielo E, Zinzi M (2013) Optical and thermal characterisation of cool asphalts to mitigate urban temperatures and building cooling demand. *Building and Environment* 60:56-65. <https://doi.org/10.1016/j.buildenv.2012.11.004>
44. Rizwan AM, Dennis LY, Chunho LIU (2008) A review on the generation, determination and mitigation of Urban Heat Island. *Journal of Environmental Sciences* 20(1):120-128. [https://doi.org/10.1016/S1001-0742\(08\)60019-4](https://doi.org/10.1016/S1001-0742(08)60019-4)

## Tables

Table 2 is not available with this version.

## Figures

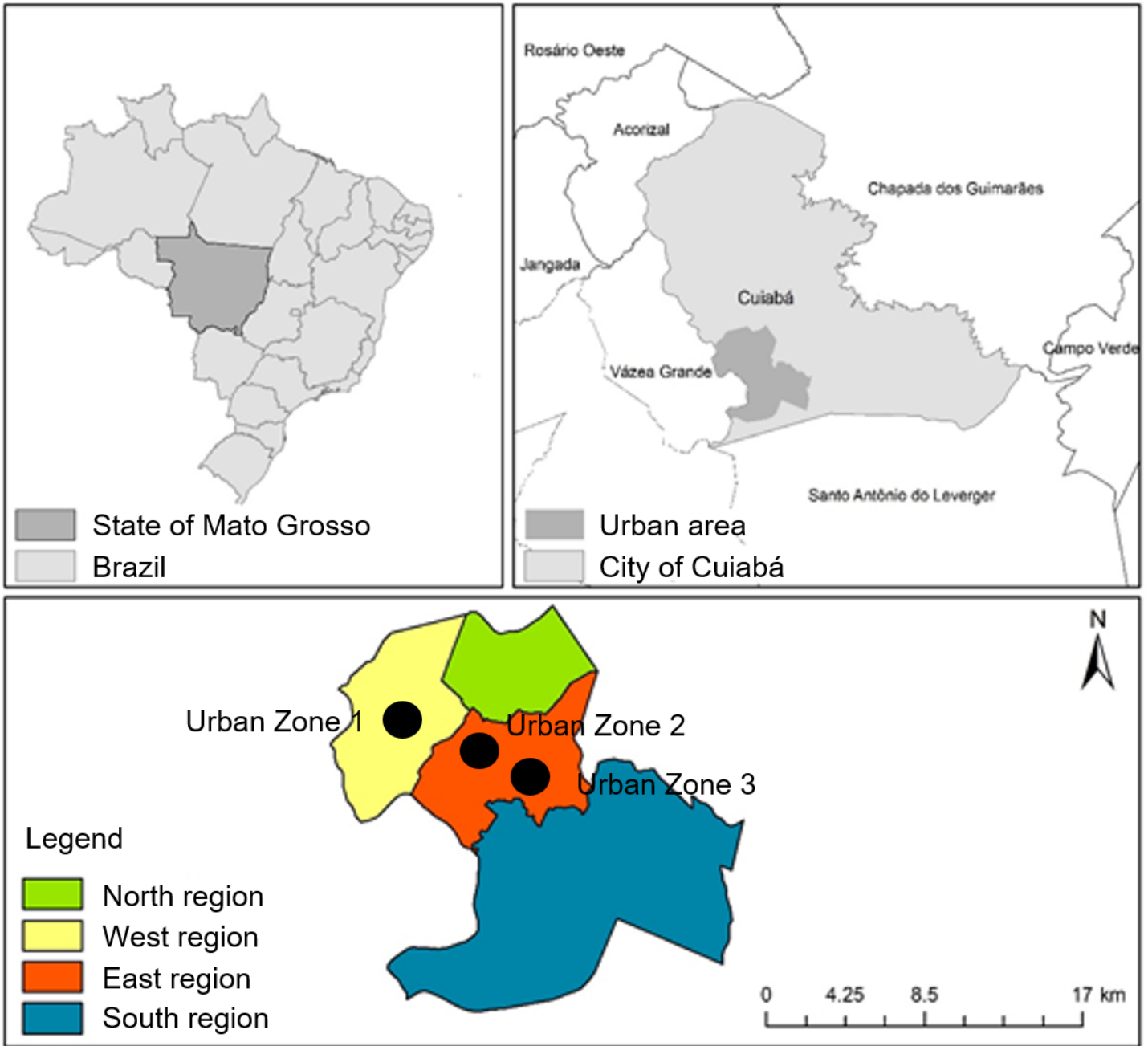


**Figure 1**

Location of the urban area of Cuiabá-MT with its administrative regions and urban zones (solid circles).

Urban Zone 1 hot-dry period



Urban Zone 1 hot-humid period



Urban Zone 2 hot-dry period



Urban Zone 2 hot-humid period



Urban Zone 3 hot-dry period



Urban Zone 3 hot-humid period



**Figure 2**

Aerial images (radius of 200 m, altitude 80 m, pixel resolution 1.25 x 1.25 cm) of Urban Zone 1, 2, and 3 captured by the DroneDeploy application during the hot-dry and hot-humid periods.

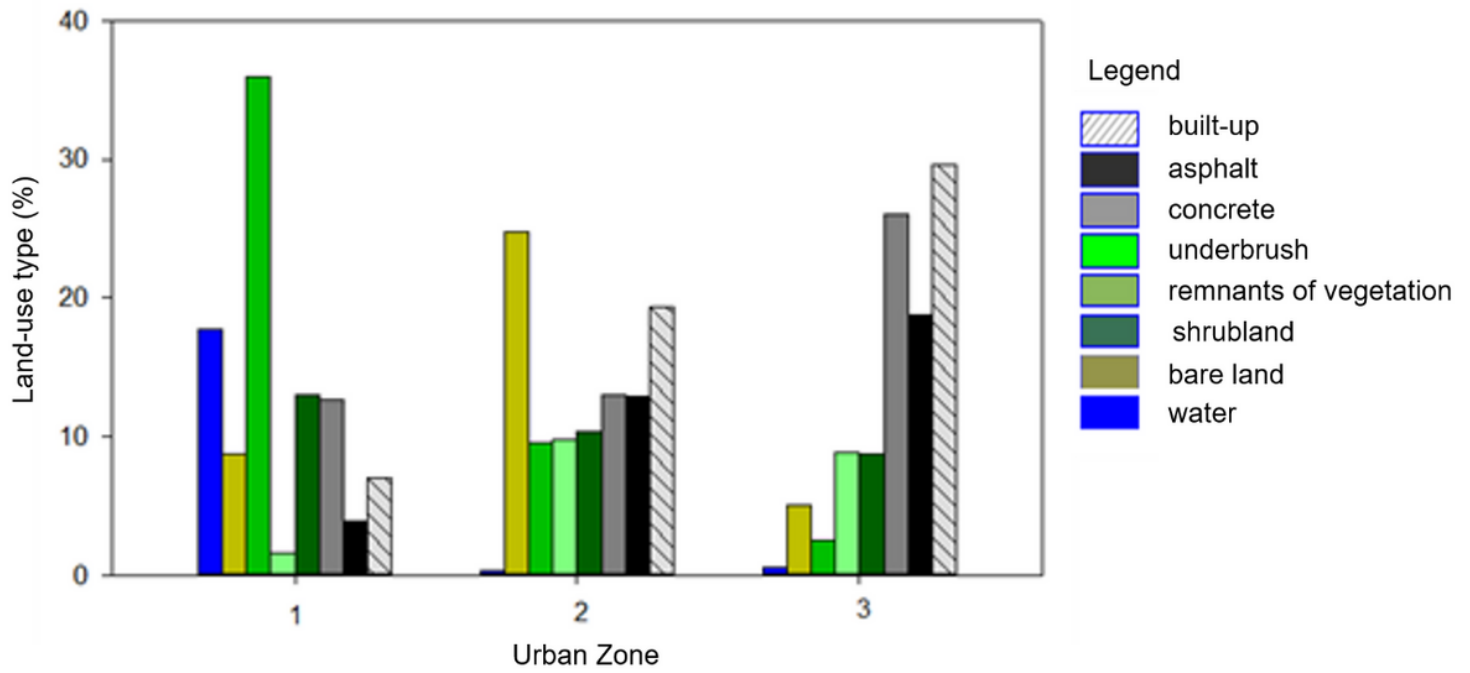


**Figure 3**

Land use class (built-up, asphalt, concrete, underbrush, remnants of vegetation, shrubland, bare land, and water) of Urban Zone 1, 2, and 3 in Cuiabá, MT, Brazil.

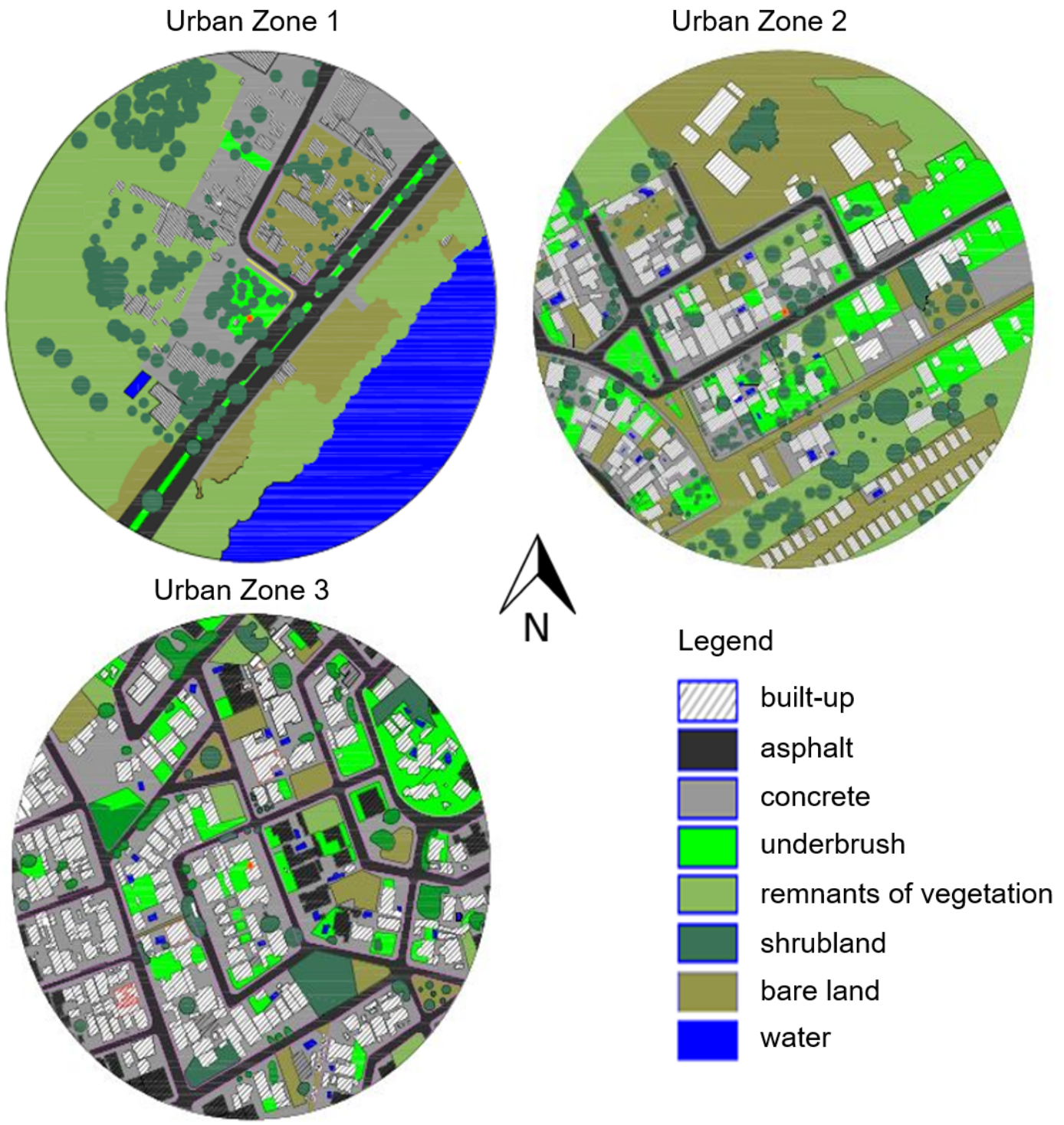


**Figure 4**

Map of the land use class (built-up, asphalt, concrete, underbrush, remnants of vegetation, shrubland, bare land, and water) of Urban Zone 1, 2, and 3 in Cuiabá, MT, Brazil.

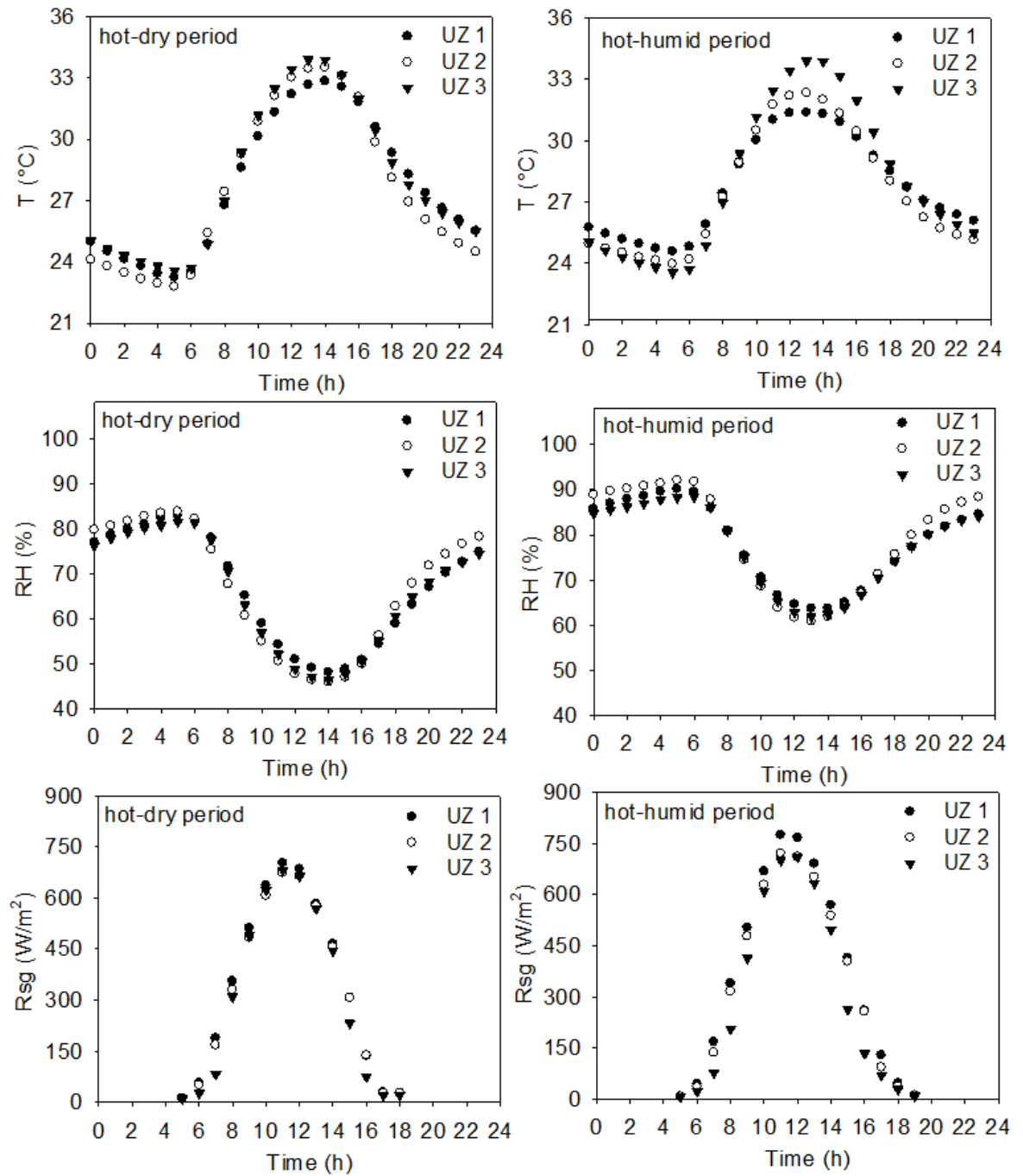


**Figure 5**

Daily cycle for each period of air temperature, relative humidity, and global solar radiation during the hot-dry and hot-humid periods in Urban Zone 1, 2, and 3 in Cuiabá, MT, Brazil.

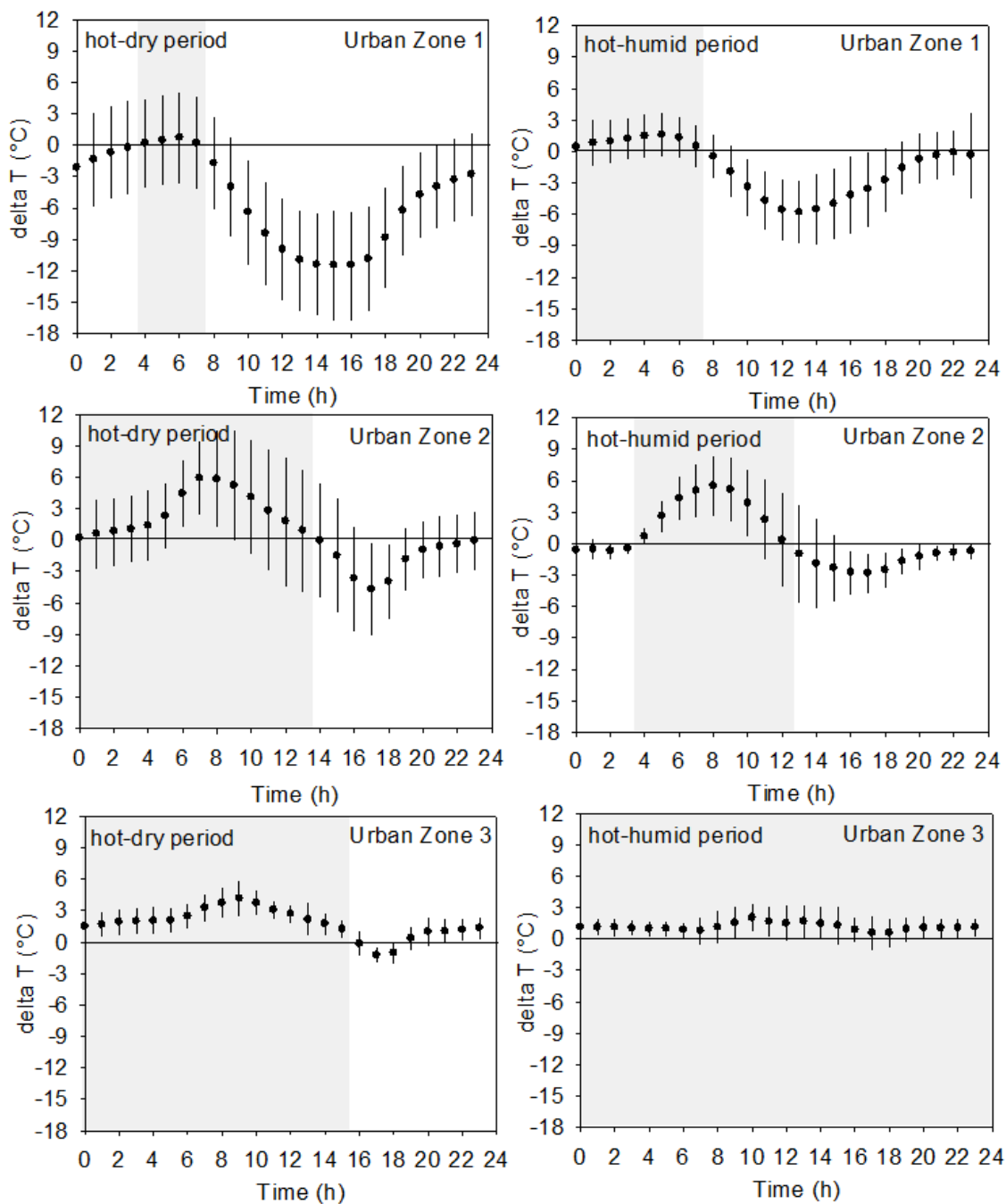


**Figure 6**

Average ( $\pm$ SD) hourly values of  $\Delta T$  (delta T, °C) in Urban Zones 1, 2, and 3 in Cuiabá, MT, Brazil. The solid line represents the limit of UHI and UCI. The shaded area represents UHI.

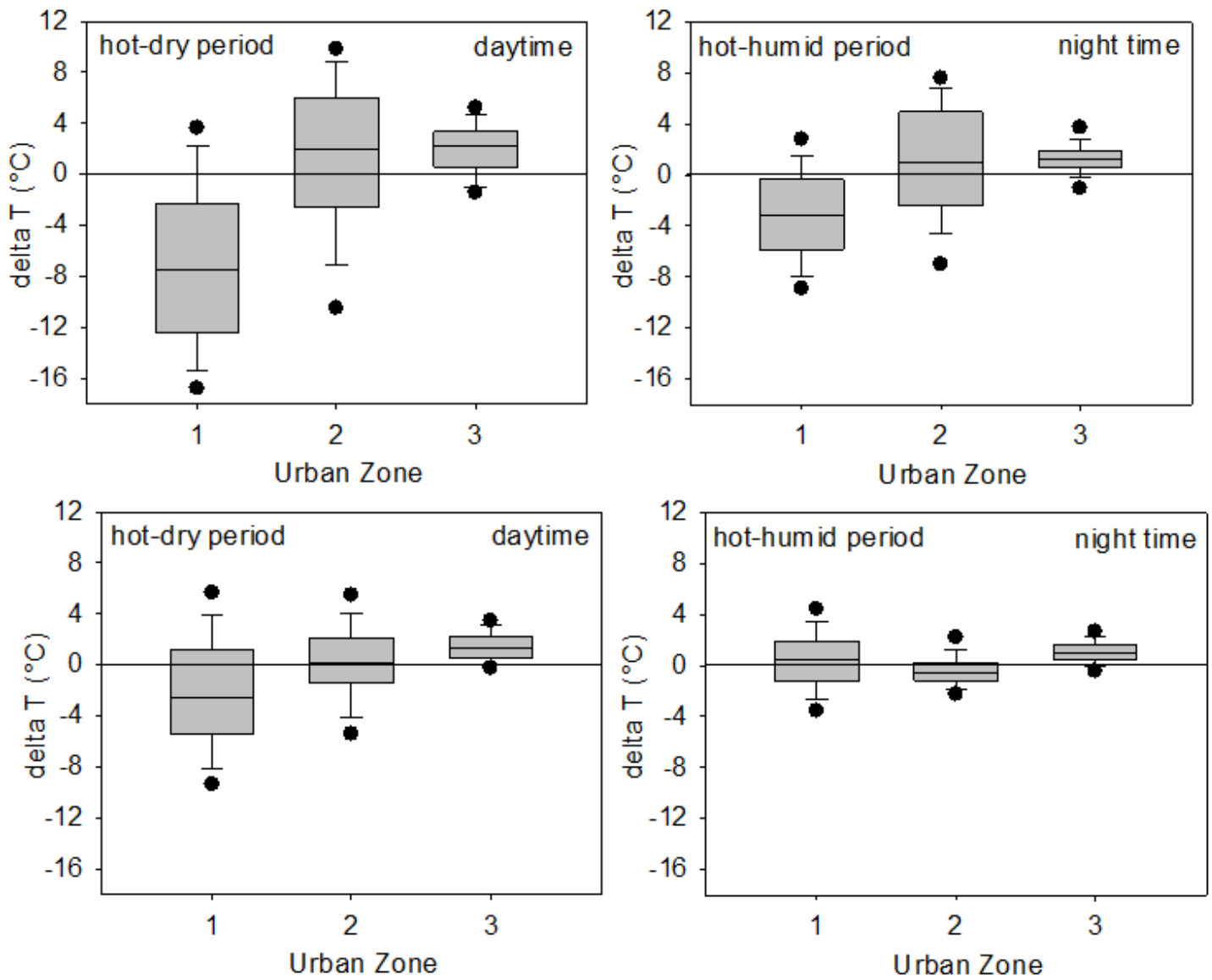


**Figure 7**

Boxplot of  $\Delta T$  (delta T, °C) of the daytime and night-time during the hot-dry and hot-humid periods in Urban Zone 1, 2, and 3 in the Cuiabá, MT, Brazil. The boxplots represent the median, 10th, 25th, 75th, and 90th percentiles as vertical boxes with error bars. The time required to calculate the daytime was from 6:00 a.m. to 6:00 p.m. (GMT-4).